



Adsorption of bisphenol A and 2,4-dichlorophenol onto cetylpyridinium chloride-modified pine sawdust: a kinetic and thermodynamic study

Hefei Wang^{1,2} · Tian Tian¹ · Dong Wang¹ · Fangdi Xu³ · Wei Ren⁴

Received: 24 July 2021 / Accepted: 18 October 2021 / Published online: 27 October 2021
© The Author(s), under exclusive licence to Springer-Verlag GmbH Germany, part of Springer Nature 2021

Abstract

Using biomass wastes as adsorbents is a promising option for organic waste reclamation, but unfortunately, their adsorption capacity is usually limited, especially for hydrophobic organic pollutants. To address this issue, this work prepared cetylpyridinium chloride (a cationic surfactant)-modified pine sawdust (CPC-PS) and further demonstrated their performance for hydrophobic bisphenol A (BPA) and 2,4-dichlorophenol (DCP) adsorption. Compared to the PS, the CPC-PS improved the maximum adsorption capacity for BPA and DCP by approximately 98% and 122%, respectively. The kinetic and thermodynamic analyses showed that the BPA and DCP adsorption onto the CPC-PS fitted the pseudo-second-order kinetics and the Freundlich model. After regeneration using NaOH, the adsorption capacity of the CPC-PS for BPA still maintained 80.2% of the initial value after five cycles. Based on the experimental results, the CPC-PS was proposed to enhance the BPA and DCP adsorption through the solubilization of hemimicelles for hydrophobic organic pollutants, the π - π stacking between benzene-ring structures, and the hydrogen binding between the adsorbents and the pollutants. This work provides a viable method to use surfactant-modified pine sawdust as effective adsorbents to remove hydrophobic pollutants.

Keywords Pine sawdust · Bisphenol A · 2,4-Dichlorophenol · Adsorption · Modification · Cetylpyridinium chloride

Introduction

The phenolic compounds are one of the commonest persistent organic pollutants in wastewaters discharged from various industries including, petrochemical engineering, timber processing, and pesticide production (Marone et al. 2016). Bisphenol A (BPA) and 2,4-dichlorophenol (DCP)

are two typical phenolic pollutants that attract widespread attention in recent years. BPA, widely used in plastic industry to produce polycarbonate and ethoxy resin, is one of the typical endocrine disrupting chemicals (Moreman et al. 2017; Vandenberg et al. 2007). DCP belongs to the chlorophenol compounds, which are difficult-biodegradable pollutants with mutagenicity and carcinogenicity (Quan et al. 2004; Sun et al. 2019). Exposure of DCP through the skin or stomach can cause serious diseases to the endocrine system (Meeker et al. 2013). During the industrial production and human activities, release of these pollutants into the environment is ineluctable, and their further accumulation will no doubt inflict a heavy damage upon all living beings (Moreman et al. 2017; Vandenberg et al. 2007).

Over the last two decades, a series of techniques, e.g., adsorption, photocatalysis, heterogeneous catalysis, solvent extraction, and biological and electrochemical degradation, have been developed to remove these phenolic pollutants from wastewater (Chen et al., 2020; Cydzik-Kwiatkowska et al. 2020; Dehghani et al. 2016; Huang et al. 2017; Jin et al. 2015; Qiu et al. 2021; Yu et al., 2020). Among these technologies, adsorption offers several

✉ Wei Ren
renvvyvan@yeah.net

- ¹ Key Laboratory of Industrial Ecology and Environmental Engineering (Ministry of Education, China), School of Environmental Science and Technology, Dalian University of Technology, Dalian 116024, People's Republic of China
- ² National Marine Environmental Monitoring Center, Dalian 116023, China
- ³ Welle Environmental Group Co., Ltd, Changzhou 213022, China
- ⁴ State Key Laboratory of Urban Water Resource and Environment, Harbin Institute of Technology, Harbin 150090, China

advantages such as simple operation, good selectivity, and strong recyclability compared to the others (Lin et al., 2021; Peng et al., 2020). To develop novel and cost-effective adsorbents with strong applicability and high performance is recognized as the key breakthrough in adsorption treatment. In recent years, natural biomass and biomass wastes including corn stalk, rice hull, peanut shell, and wood filings are gradually used as low-cost adsorbents in their natural forms or physiochemically modified forms, to separate heavy metals and organic pollutants from wastewater (Mpatani et al. 2021). These natural adsorbents are biodegradable, renewable, biocompatible, and nontoxic.

Pine sawdust (PS), the by-products in wood and furniture industry, have been successfully used as adsorbents, because they contain a large number of carboxyl, hydroxyl, and acylamino groups (Jung et al. 2013; Neris et al. 2019). However, the adsorption capability of PS for organic pollutants is somewhat hampered. To address these issues, researchers have made large efforts to enhance the adsorption capability of PS by modifying with citric acids (Zhou et al. 2015), EDTA dianhydride (Pereira et al. 2010), polyaniline (Nasar and Mashkour, 2019), and etc. For organic pollutants, especially hydrophobic compounds, using cationic surfactants to modify PS to promote their adsorption performance is an effective strategy, but unfortunately, the related available information is still limited. When the concentration of surfactant exceeds its critical micelle concentration, micellar aggregates with a hydrophobic core and a hydrophilic surface are formed (Nagarajan and Ruckenstein, 1991; Santos and Panagiotopoulos, 2016). The micellar aggregates can enhance the “water solubility” (dissolved in the micelle) of insoluble or slightly soluble organics, which is also known as the micelle solubilization (Li et al. 2019; Mousset et al. 2014; Patel et al. 2017). Through micelle solubilization, the surfactant-modified adsorbents hold a promising tool to treat hydrophobic organic pollutants, such as BPA and DCP.

Therefore, the main objective of this work was to use a cationic surfactant (cetylpyridinium chloride, CPC) to modify the PS as adsorbents, and to evaluate their adsorption performance for BAP and DCP removal. The CPC-modified PS were finely characterized and their adsorptive ability for BAP and DCP were investigated. In addition, the key factors (e.g., adsorption time, pH, adsorbent dosage, temperature, and ionic strength) influencing the adsorption process were also studied. Finally, the kinetic and thermodynamic analyses were performed, and an underlying adsorption mechanism was correspondingly proposed to get a further insight into the BPA and DCP adsorption process. This work provides a viable method to use surfactant-modified biomass wastes as an effective adsorbent for pollutant removal.

Materials and methods

Chemicals

Cetylpyridinium chloride (CPC, 99%) and bisphenol A (BPA, A.R.) were purchased from Sinopharm Chemical Reagent Co., Ltd., China. 2,4-Dichlorophenol (DCP, 99%) was purchased from J&K Scientific Ltd., China. Pine sawdust (200-mesh) were acquired from a lumber mill located in Guangzhou, China. Other chemicals used in this work including, methanol, ethanol, and NaOH were all analytical reagents.

Preparation of modified pine sawdust

Before modification, the raw pine sawdust (PS) was first pretreated using ethanol to remove the soluble impurities. Briefly, the PS (25 g) were added into 250 mL of ethanol and then vibrated at 150 rpm, 50 °C for 4 h. Left precipitated for 4 h, the solid PS were collected by vacuum filtration. Subsequently, the soluble impurities on the surface of PS were rinsed three times with ethanol, followed by washed with deionized water until the filtrate turned colorless. After dried at 105 °C for 24 h, the precipitates were finely milled and stored in a vacuum desiccator. The pretreated PS with a total weight of 0.5 g were added into 50 mL of CPC solutions with given concentrations of 0.2, 0.4, 1.0, 5.0, and 10.0 g/L. Then, the mixtures were vibrated at 150 rpm, 50 °C for 12 h. After solid–liquid separation through vacuum filtration, the precipitates were rinsed with ethanol and deionized water in turn until no surfactant dissolution was measured. The modified PS with 0.2, 0.4, 1.0, 5.0, and 10 g/L of CPC were named as CPC-PS1, CPC-PS2, CPC-PS3, CPC-PS4, and CPC-PS5, respectively. Afterwards, the modified PS were fully dried at 80 °C for 24 h, finely milled, and stored in a vacuum desiccator for further use. Pre-adsorption of BPA and DCP (100 mg/L) was carried out using the PS and CPC-PS, respectively.

Characterization of adsorbents

The PS and CPC-PS were characterized using scanning electron microscopy (SEM, Quanta 450, FEI, USA) and Fourier transform infrared spectroscopy (FT-IR, Equinox 55, Bruker, Germany). Brunauer–Emmett–Teller analysis (BET, Tristar II 3020 M, Micromeritics, USA), thermogravimetric analysis (TGA, SDT Q600, TA, USA), and elemental composition analysis (Vario EL cube, Elementar, Germany) of these adsorbents were also performed. FT-IR spectra were conducted using the KBr pressed-disk methods with a spectral scanning range from 400 to 4000 cm^{-1} with air as the

background. BET surface area was measured under N₂ conditions after desorption for 12 h at room temperature. TGA analysis was conducted by adding 5.09 g of PS and 4.49 g of CPC-PS into crucibles and heated from 39 to 800 °C (10 °C/min) under N₂ conditions (100 mL/min).

Batch adsorption experiments

Sacrificial batch adsorption experiments were conducted by adding 0.03 g PS and CPC-PS into 20 mL of BPA and DCP solutions (100 mg/L), respectively. Samples were collected at the given time intervals (2, 4, 6, 8, 10, 15, 20, 30, 60, 90, 120, 150, and 180 min), and filtrated with 0.45 µm PES membranes to determine the residual concentrations of BPA and DCP and to calculate the kinetic parameters. To investigate the potential effects of pH and ion strength on the adsorption performance, a series of sacrificial batch adsorption tests were performed under different pH and ion strength conditions. The initial pH of both BPA and DCP solutions were adjusted to 2.0, 3.0, 4.0, 5.0, 6.5, 8.0, 9.0, 10.0, 11.0, and 12.0 with either HCl or NaOH. In addition, to discuss the effect of ion strength on adsorption process, tests were also carried out in the BPA and DCP solutions containing 0, 0.05, 0.1, 0.15, 0.2, and 0.25 M of NaCl. All the batch experiments were performed by vibration at 150 rpm, 25 °C for 3 h to achieve adsorption equilibrium. The residual BPA and DCP were quantified using a spectrophotometer (V-560 UV/VIS Spectrophotometer, Jasco, Japan) at 275 nm and 285 nm, respectively (Cheng et al. 2012; Yin and Shang, 2020).

To explore the effect of different dosages of adsorbents on BPA and DCP removal, a total weight of PS and CPC-PS from 0.02 to 0.3 g was added into 20 mL and 100 mg/L of BPA and DCP solutions. At the meantime, adsorptions of BPA (20, 40, 60, 80, 100, 125, and 150 mg/L) and DCP (25, 50, 100, 150, 200, 250, and 300 mg/L) were also conducted using 0.03 g PS and CPC-PS to demonstrate the differences in adsorption performance at different initial concentrations. The adsorption tests were performed by vibration for 3 h at 150 rpm and 25, 35, and 45 °C, respectively. The residual concentrations of BPA and DCP were measured, and the isothermal adsorption curves were fitted for further thermodynamic calculations. The sacrificial batch experiments were carried out in triplicate, and the results presented are the mean values.

Regeneration experiments

Regeneration of the CPC-PS for BPA adsorption was tested to investigate the applicability of the modified adsorbents. A total weight of 0.15 g CPC-PS was adopted to remove 100 mg/L of BPA. The adsorption process was carried out at 25 °C, 150 rpm for 3 h. Subsequently, the CPC-PS were

collected via vacuum filtration and regenerated by dissolved in a NaOH solution (1.0 M) and vibrated for 2.5 h. After the regeneration treatment, the adsorbents were dried at 105 °C in an oven for 5 h, followed by finely milled again for the next adsorption experiments.

Results and discussion

Adsorption pretreatment

Figure 1 illustrates the adsorption curve of CPC onto PS at 50 °C. Within an initial concentration range from 0.1 to 0.5 g/L, the CPC adsorption increased rapidly from 20.0 to 67.6 mg/g. Subsequently, the adsorption amount increased from 67.6 to 96.9 mg/g at a relatively lower rate (CPC concentration between 0.5 and 2.0 g/L). A further increase in CPC concentration up to 5.0 g/L only induced a slight adsorption increment to 107.2 mg/g, which was close to the saturated adsorption amount. Based on the above results, this work further modified PS with 0.2, 0.4, 1.0, 5.0, and 10.0 g/L of CPC, respectively.

Table 1 shows the BPA and DCP adsorption onto the PS and the CPC-PS. Compared to PS, the CPC-PS exhibited higher adsorption capacities for both BPA (from 12.5 to 24.6 mg/g) and DCP (from 5.2 to 12.5 mg/g). Among the CPC-PS, the CPC-PS4 showed the optimal performance, and thus, it was chosen for further investigations.

The Zeta potential of the PS was −23.1 mV. After modification, the Zeta potential of the CPC-PS was gradually improved with increasing initial CPC concentrations (Table 1). When CPC was below its critical micelle concentration, it mainly existed in ionic form, which might increase Zeta potential by electrostatic attraction (Ge et al. 2015;

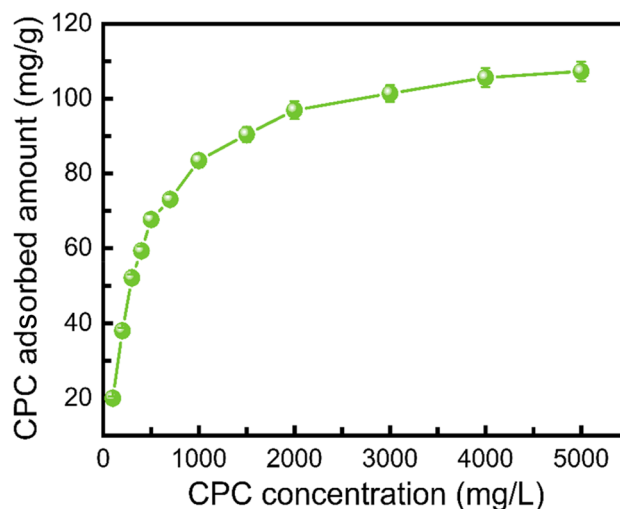
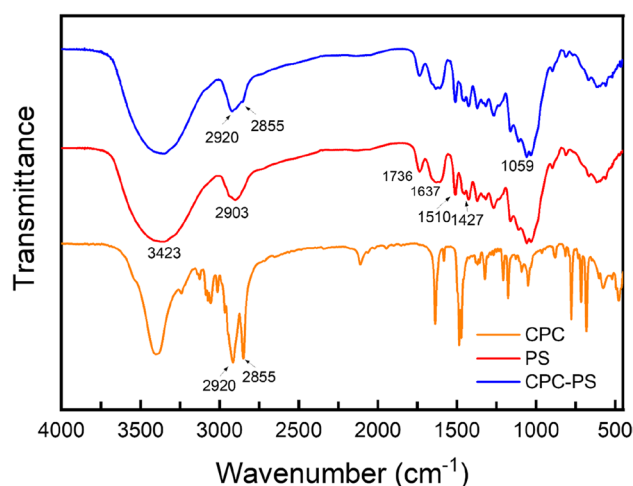


Fig. 1 Adsorption isotherm curve of the CPC adsorption onto PS

Table 1 Characterizations of the adsorbents and pre-adsorption of BPA and DCP

Adsorbent	N (%)	C (%)	H (%)	S (%)	Zeta potential (mV)	BET (m ² /g)	q _{BPA} (mg/g)	q _{DCP} (mg/g)
PS	0.11	46.74	6.10	0.063	−23.1	4.11	12.5	5.3
CPC-PS1	0.20	47.58	6.26	0.073	−20.7		17.6	8.2
CPC-PS2	0.26	48.17	6.35	0.030	−19.7	3.76	23.0	11.3
CPC-PS3	0.25	48.47	6.28	0.032	−18.2		24.0	12.2
CPC-PS4	0.24	48.50	6.30	0.044	−17.2	3.78	24.6	12.5
CPC-PS5	0.25	48.48	6.38	0.022	−16.8		24.3	12.2

Note: PS pine sawdust; CPC-PS1 ~ CPC-PS5 CPC-modified PS with 0.2, 0.4, 1.0, 5.0, and 10 g/L PS

**Fig. 2** FT-IR spectra of the PS, CPC, and the CPC-PS

Koopal et al. 2004). The surface areas of PS, CPC-PS2, and CPC-PS4 were 4.11, 3.76, and 3.78 m²/g respectively, indicating a slight decrease in the surface area of PS after modification. The elemental composition analysis showed the contents of C and N of these adsorbents increased from 46.7% and 0.11% to 48.5% and 0.25% with increasing CPC concentrations. Because the CPC contained long-chain alkyl groups and pyridine, such improvements in C and N contents could also indicate the successful loading of CPC onto PS (Ibrahim et al. 2009).

Characterization of adsorbents

The FT-IR spectra of the PS, CPC, and the CPC-PS are illustrated in Fig. 2. The FT-IR spectrum of the PS shows a clear band at 3423 cm^{−1}, which is the stretching vibration of O–H, and the bands between 2975 and 2800 cm^{−1} are associated with the stretching vibration of C–H, including CH, CH₂, and CH₃ (Kumar et al. 2018; Ren et al. 2020). The band at 1736 cm^{−1} is the stretching vibration of C=O, most likely from ketone carbonyl group and esters (Pereira et al 2010; Zhou et al. 2015). The bands at 1637 and 1510 cm^{−1} are the stretching vibration of C=O

belonging to carboxyl or acylamino and the bending vibration of N–H belonging to amidogen or acylamino (Semerjian, 2018). The band at 1427 cm^{−1} shows the deformation vibration of C–OH, while the band at 1059 cm^{−1} is the stretching vibration of C–O–C, which might result from the existence of substantial lignin in the PS (Tian et al. 2020). In comparison, the CPC-PS show basically the same characteristic bands with several slight changes. The band at 2903 cm^{−1} is shifted and divided into two characteristic bands at 2920 and 2855 cm^{−1}. The bands between 2975 and 2800 cm^{−1} are still the stretching vibration of C–H, but the band at 2920 cm^{−1} is the asymmetrical stretching vibration of CH₂ and the band at 2855 cm^{−1} is the symmetrical stretching vibration of CH₂. Such a difference could be ascribed to the intervention of the alkyl chain of CPC, which underscored again the loading of CPC onto PS.

Figure 3A displays the thermogravimetric curve of the PS, where two obvious thermal decomposition peaks at 58 °C (40~100 °C) and 366 °C (250~400 °C) could be observed. Based on these data, the pyrolysis of PS could be divided into three phases. In phase I (38~96 °C), physical processes such as surface moisture evaporation occurred with a mass loss of 4.8%. Pyrolysis of lignin and cellulose in PS took place in phase II, which resulted in a total mass loss of 68.2%. Finally, in phase III (400~800 °C), a secondary pyrolysis of the pyrolysis products generated in phase II was observed with a mass loss of 12.0%. The thermogravimetric curve of the CPC-PS also shows two obvious thermal decomposition peaks at 53 °C and 373 °C. The mass loss of the CPC-PS in phase I was calculated to be 4.3%, less than that of the PS. A reasonable explanation for this difference was that the CPC modification changed the hydrophilicity of PS, which further reduced the surface moisture content (Jiang et al., 2020; Zhou et al. 2017). The mass loss in phase II was 70.3%, and a small thermal decomposition peak between 250 and 300 °C appeared. Such changes in phase II could be attributed to the intervention of CPC. Since the main compositions of CPC and PS were all carbohydrates, it was not appropriate to calculate the loading capacity of CPC using the quality difference of TGA.

Fig. 3 TGA curves of the PS (A) and the CPC-PS (B)

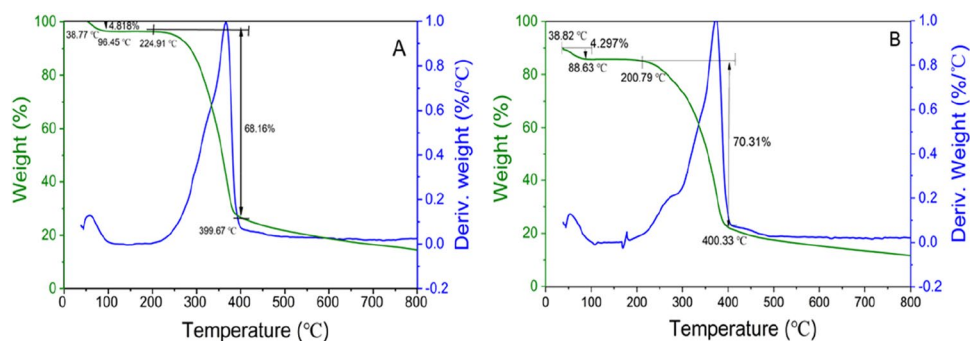
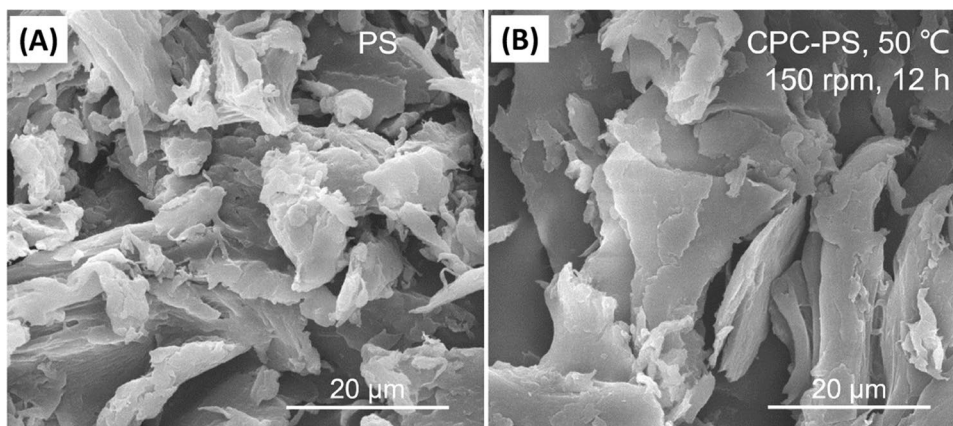


Fig. 4 SEM images of the PS (A) and the CPC-PS (B)



The morphology of the PS and the CPC-PS displayed a certain difference, but not significantly. The SEM image of the PS shows a coarse fiber-like texture, while the surface of the CPC-PS exhibited a relatively smooth morphology (Fig. 4).

Effect of contact time on BPA and DCP adsorption

Figure 5 shows the time course of the BPA and DCP adsorption onto the CPC-PS. BPA was rapidly adsorbed onto the CPC-PS with the adsorption capacity soaring to 21.2 mg/g within 15 min. Then, the adsorption rate slowed down at the next stage (15 ~ 90 min), and the BPA adsorption capacity further increased to 24.0 mg/g. Finally, the BPA adsorption tended towards equilibrium from 90 to 180 min. The DCP adsorption onto the CPC-PS was similar to that of BPA. The adsorption capacity for DCP soared to 11.3 mg/g within 10 min, and then slowly to 12.4 mg/g from 10 to 60 min. The adsorption equilibrium was gradually achieved from 60 to 180 min with an equilibrium adsorption capacity of 12.4 mg/g. In comparison, the equilibrium adsorption capacity for BPA was 24.1 mg/g, which demonstrated a superior adsorption of BPA onto the CPC-PS. Moreover, the CPC-PS synthesized in this work also showed a superior BPA adsorption than previous reports using β -cyclodextrin-modified

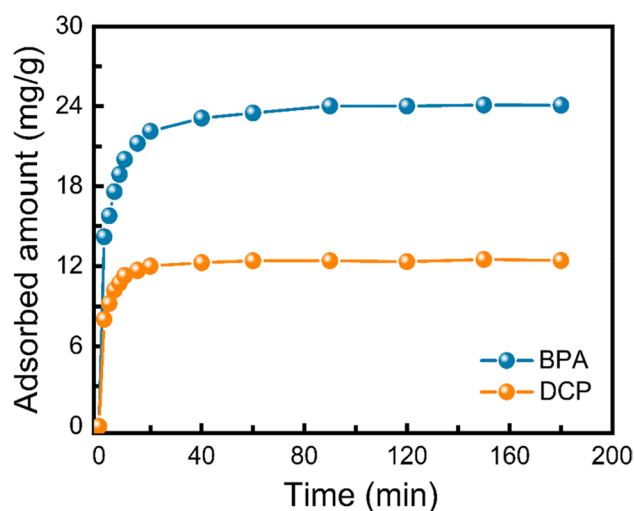


Fig. 5 Time course of BPA and DCP adsorption onto the CPC-PS

PS (Zhou et al., 2017), or surfactant-modified natural clays (Berhane et al., 2016; Li et al., 2015).

To better analyze the adsorption properties of BPA and DCP onto the CPC-PS, this work further investigated their adsorption kinetics based on the above data. Table 2 displays the related parameters of the pseudo-first-order and pseudo-second-order kinetic models for BPA and DCP

Table 2 Parameters of the kinetic models

Pollutants	$q_{e,exp}$ (mg/g)	Pseudo-first-order kinetics			Pseudo-second-order kinetics		
		k_1 (min ⁻¹)	$q_{e,cal}$ (mg/g)	R^2	k_2 (g mg ⁻¹ min ⁻¹)	$q_{e,cal}$ (mg/g)	R^2
BPA	24.1	0.297	22.9	0.936	0.022	24.2	0.990
DCP	12.4	0.411	12.0	0.967	0.063	12.6	0.997

Pseudo-first-order kinetics: $q_t = q_e[1 - e^{-k_1t}]$

Pseudo-second-order kinetics: $q_t = \frac{k_2q_e^2t}{1+k_2q_e t}$

adsorption. It could be noted that both the BPA and DCP adsorption process fitted the pseudo-second-order kinetics better ($R^2 = 0.990$ and 0.997 , respectively). Moreover, the difference between the $q_{e,cal}$ obtained from the pseudo-second-order kinetics and the experimentally measured $q_{e,exp}$ was slight.

Effect of initial solution pH on BPA and DCP adsorption

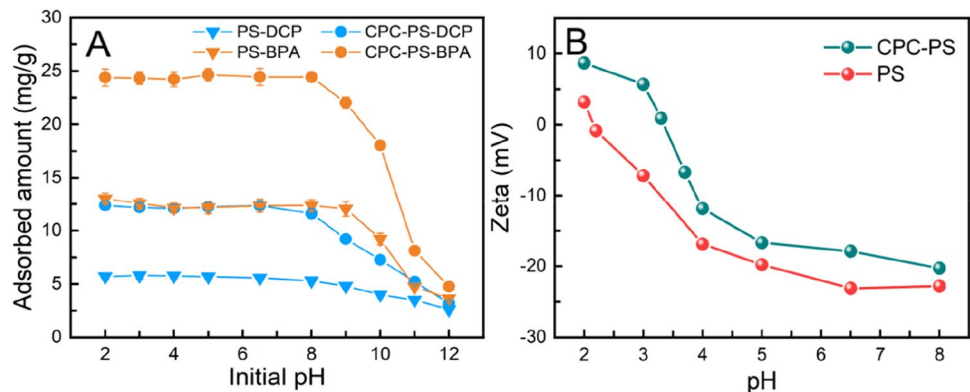
To demonstrate the effect of initial solution pH on BPA and DCP adsorption, a series of BPA and DCP solutions at a pH range of 2.0 to 12.0 were prepared. At a pH range between 2.0 and 8.0, the BPA adsorption onto the PS and the CPC-PS kept relatively unchanged with an adsorption capacity of 12.4 and 24.5 mg/g, respectively (Fig. 6A). As pH increased to 12.0, the adsorption capacity of the PS and the CPC-PS for BPA dropped sharply to 3.6 and 4.8 mg/g. A similar trend for the DCP adsorption onto the PS and the CPC-PS was also observed at different initial pH. At a pH range of 2.0 to 6.5, the adsorption capacities of the PS and the CPC-PS for DCP were measured as approximately 5.6 and 12.4 mg/g. However, when the pH increased to 12, the adsorption capacity plunged to 2.6 mg/g (PS) and 3.2 mg/g (CPC-PS), respectively. These results suggested that the adsorption capacity of the PS and the CPC-PS for BPA and DCP could remain relatively stable under acidic conditions, but their performance deteriorated significantly under alkaline conditions. In comparison, the BPA adsorption capacity

of the CPC-PS was promoted by 98%, and for DCP, it was promoted by 122%.

Figure 6B shows the Zeta potential of the PS and CPC-PS at different pH. The parameter pH_{PZC} , which was the pH of a solution when the net surface charge was zero (Ayranci and Duman, 2006), was introduced to analyze the relationship between pH and the Zeta potential of these adsorbents. The pH_{PZC} of PS was measured to be 2.2, indicating a positive Zeta potential of PS when $pH < 2.2$. Under such circumstances, the BPA and DCP were in their molecular forms. When $pH > 2.2$, the Zeta potential of PS turned negative. After modification, the Zeta potential of CPC-PS showed an obvious increase, and the pH_{PZC} of CPC-PS increased to 3.3. The PS offered carboxyl, hydroxyl, and acylamino groups that could attract BPA and DCP through hydrogen bonding (Jang et al. 2018). The enhanced adsorption capacity of CPC-PS could be attributed to the combination of the solubilization of CPC (Rehman et al. 2020) and the surface adsorption by PS.

Compared to DCP, the BPA adsorption exhibited a stronger resistance to the pH variation, mainly resulted from the different pK_a values of BPA and DCP. Both the BPA and DCP were dissociated organics with a pK_a value of 9.60 and 7.89, respectively (Ololade et al. 2018). When the pH was close to or beyond their pK_a values, the BPA and DCP were gradually dissociated into anionic forms, causing a decline in their hydrophobicity. As a result, both the BPA and DCP adsorption onto the PS and the CPC-PS were seriously inhibited under alkaline conditions. In addition, the

Fig. 6 Effect of initial pH on BPA/DCP adsorption onto the PS and the CPC-PS (A), and Zeta potential of the adsorbents at different pH (B)



surfaces of the PS and the CPC-PS were also negatively charged, which would repulse the BPA and DCP anions and lead to a further decline in their adsorption capacity.

Effect of ionic strength on BPA and DCP adsorption

Practical wastewater usually contains a certain number of salts, and thus, the effect of ionic strength on BPA and DCP adsorption should not be overlooked. In this work, the effect of ionic strength on BPA and DCP adsorption was investigated with NaCl (0~0.25 M) as a typical example (Fig. 7). As the NaCl concentration increased, the adsorption capacities of the PS for BAP and DCP were first promoted from 12.3 and 5.4 mg/g to 14.8 and 6.2 mg/g, and then dropped to 13.1 and 5.4 mg/g, respectively. In comparison, the adsorption capacities of the CPC-PS were first improved from 24.4 (for BPA) and 12.2 (for DCP) mg/g to 25.7 and 13.1 mg/g, and then declined to 24.6 and 12.1 mg/g. The increase in the ionic strength could compress the electrical double layer, which would further enhance the interactions between surfactants and pollutants (Che Man et al. 2014). Generally, the ionic strength showed a limited impact on the BPA and DCP adsorption onto the PS and the CPC-PS.

Effect of adsorbent dosage on BPA and DCP adsorption

Figure 8 illustrates that the removal efficiency of either BPA or DCP was improved as the adsorbent dosage increased. With 1~10 g/L PS or CPC-PS supplemented, the BPA removal efficiency was improved from 14.7% (PS) and 25.6% (CPC-PS) to 63.6% and 83.4%, while the removal efficiency of DCP increased from 6.5% (PS) and 15% (CPC-PS) to 45.1% and 71.0%, respectively. At a dosage range of 10–15 g/L, the adsorption rate of both the PS and the

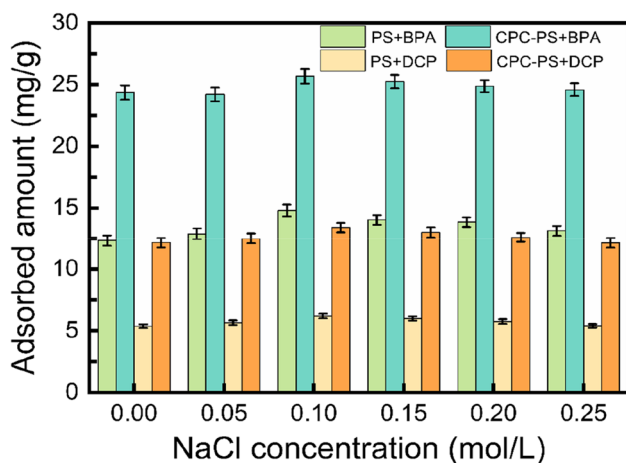


Fig. 7 Effect of ionic strength on BPA and DCP adsorption onto the PS and the CPC-PS

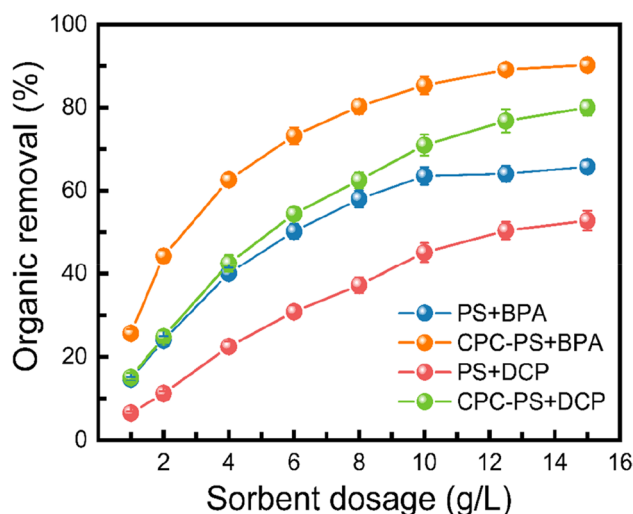


Fig. 8 Effect of adsorbent dosage on BPA and DCP adsorption onto the PS and the CPC-PS

CPC-PS slowed down with a final BPA removal efficiency of 65.8% and 90.2%, and a final DCP removal efficiency of 52.8% and 80%. The BPA adsorption showed a superior performance compared to the DCP adsorption, which might be ascribed to a higher hydrophobicity of BPA (Log *o/w* of 3.30) than DCP (Log *o/w* of 3.09) (Ding et al. 2016; Joseph et al. 2011). The above results clearly corroborated the enhanced BPA and DCP adsorption onto the CPC-PS. Considering the pollutant removal and the adsorbent utilization efficiency, the optimal adsorbent dosage was chosen as 10 g/L.

Effect of temperature on BPA and DCP adsorption

Figure 9 illustrates the isothermal adsorption curves of BPA and DCP adsorption onto the PS and the CPC-PS at 25, 35, and 45 °C. The initial concentrations of BPA and DCP were set between 20~150 and 25~300 mg/L, respectively. The adsorption capacity for either BPA or DCP was enhanced with increasing initial concentrations. Compared to the PS, the CPC-PS exhibited a superior adsorption performance. It was interesting that the adsorption of BPA and DCP showed opposite trends in response to the temperature changes. As the temperature increased, the adsorption capacity of the CPC-PS for BPA was reduced, while it was enhanced for DCP. Such opposite trends might be caused by the differences in the thermodynamic properties of BPA and DCP adsorption process, which were discussed later.

Subsequently, the adsorption isothermal model of BPA and DCP adsorption onto the PS and the CPC-PS was fitted using Langmuir, Freundlich, and linear model, respectively (Table 3). It could be noted that both the BPA and DCP adsorption onto the PS and the CPC-PS fitted well

Fig. 9 Adsorption isotherms of BPA (a, c, e) and DCP (b, d, f) onto the PS and the CPC-PS

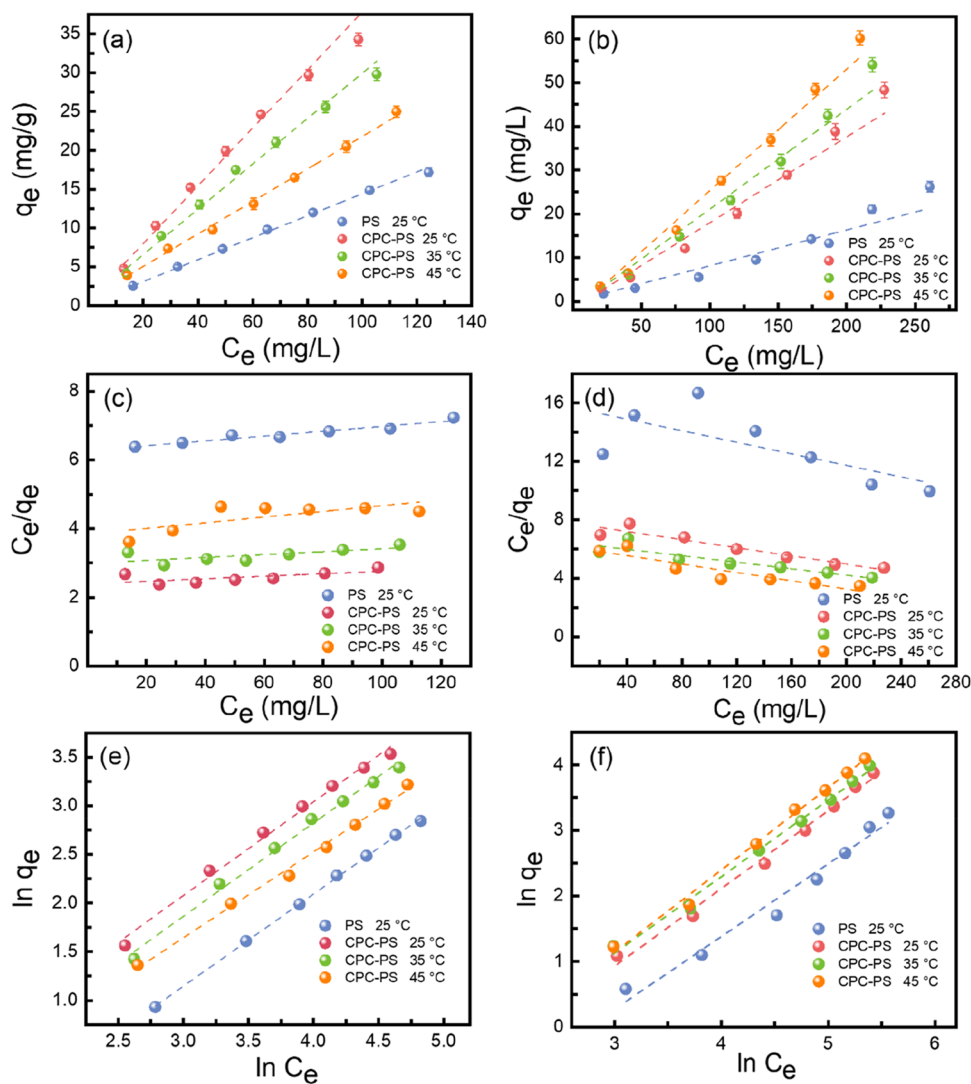


Table 3 Parameters of the adsorption isotherms of BPA and DCP adsorption onto the PS and the CPC-PS

Adsorption	T (°C)	Langmuir model			Freundlich model			Linear model		
		q_m	K_L	R^2	n	K_f	R^2	K_d	b	R^2
PS + BPA	25	142.9	0.0011	0.936	1.06	0.18	0.999	0.14	0.57	0.998
CPC-PS + BPA	25	270.3	0.0015	0.429	1.04	0.45	0.992	0.34	1.86	0.990
	35	238.1	0.0014	0.481	1.04	0.36	0.994	0.28	1.49	0.992
	45	120.5	0.0022	0.522	1.13	0.37	0.995	0.21	0.71	0.997
PS + DCP	25	50.5	0.0013	0.505	0.90	0.047	0.974	0.10	-2.43	0.970
CPC-PS + DCP	25	71.4	0.0018	0.911	0.84	0.072	0.992	0.22	-4.20	0.987
	35	90.9	0.0017	0.825	0.86	0.093	0.993	0.25	-4.06	0.988
	45	70.4	0.0023	0.840	0.80	0.073	0.995	0.30	-5.00	0.994

to the Freundlich and linear models. In comparison, the BPA adsorption showed a relatively higher correlation coefficient than that of the DCP adsorption. The Freundlich constant n was close to 1, indicating that the distribution effect of adsorbents on BPA and DCP played an important role during adsorption. Since the PS contained

carboxyl, hydroxyl, acylamino groups and a series of binding sites with BPA and DCP (e.g., hydrogen bond), the BPA and DCP adsorption onto the CPC-PS belonged to a heterogeneous adsorption of multi-molecular layers. In addition, the Freundlich constant n of the BPA adsorption

Table 4 Thermodynamic parameters of BPA and DCP adsorption onto the PS and the CPC-PS

Adsorption	T (°C)	ΔG kJ mol ⁻¹	ΔH kJ mol ⁻¹	ΔS J mol ⁻¹ K ⁻¹
PS+BPA	25	-12.2		
CPC-PS+BPA	25	-14.5	-18.9	-14.9
	35	-14.4		
	45	-14.2		
PS+DCP	25	-11.5		
CPC-PS+DCP	25	-13.4	12.2	85.8
	35	-14.2		
	45	-15.1		

Table 5 Reusability of the CPC-PS for BPA removal

Cycles	1	2	3	4	5
Adsorptive capacity (mg/g)	24.3	22.3	21.7	20.8	19.5

was higher than that of the DCP adsorption, suggesting a favorable adsorption of BPA onto these adsorbents.

Table 4 elaborates the thermodynamic properties including the Gibbs free energy (ΔG), enthalpy change (ΔH), and entropy change (ΔS) of the BPA and DCP adsorption. At the given temperatures, the ΔG of BPA and DCP adsorption onto both the PS and the CPC-PS were negative. The ΔH of BPA adsorption onto the CPC-PS was -18.9 kJ/mol, while it was 12.2 kJ/mol for the DCP adsorption. These results were consistent with the different adsorption performance in response to the temperature changes, indicating that the effect of temperature on BPA and DCP adsorption onto the CPC-PS differed. In addition, the ΔS of BPA adsorption onto the CPC-PS was -14.9 J/mol/K, suggesting a decrease in the degree of freedom during adsorption. However, the ΔS of DCP adsorption onto the CPC-PS was 85.8 J/mol/K, which demonstrated an increase in the degree of disorder during this process.

Recycling of adsorbents

To investigate the applicability of the CPC-PS, recycling experiments of BPA adsorption were conducted to measure the changes in adsorption performance. The regeneration of adsorbents was achieved by treating with NaOH solution, and the recycling experiments were performed for 5 rounds. It could be seen in Table 5 that after 5 cycles of adsorption and regeneration, the CPC-PS still held a BPA adsorption capacity of 19.5 mg/g, which was 80.2% of the initial value. These results suggested that the CPC-PS had a sufficient mechanical strength and stability during the adsorption and regeneration cycles.

Proposed adsorption mechanism

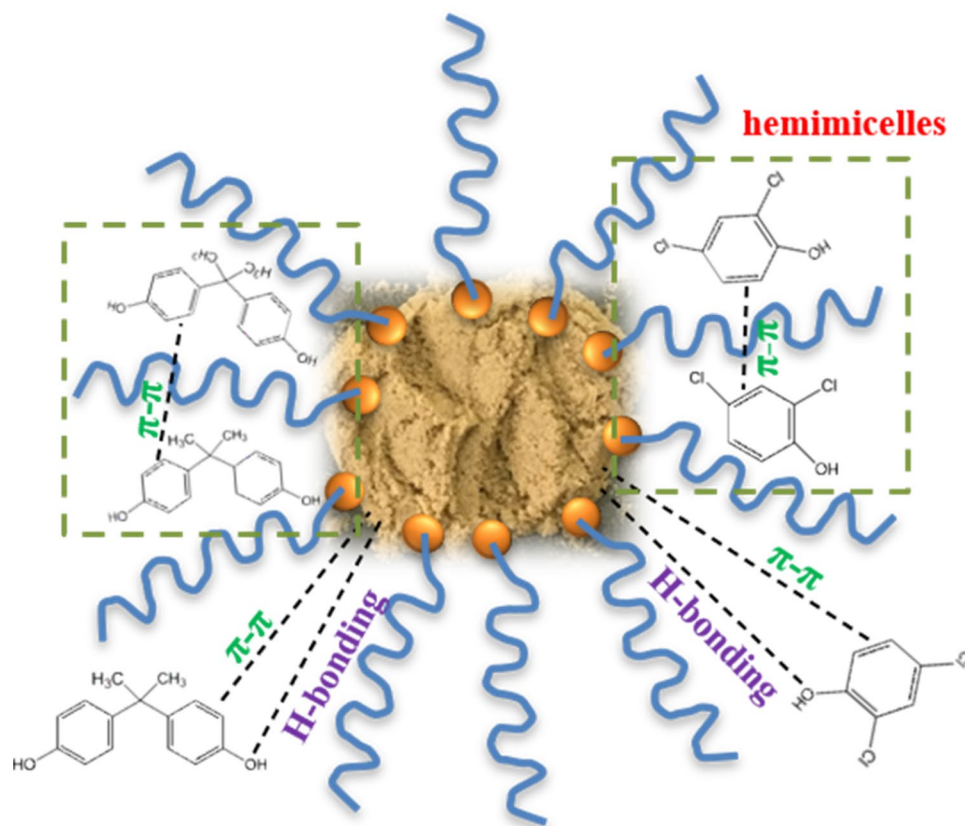
According to the aforementioned results, an underlying mechanism of BPA and DCP adsorption onto the CPC-PS was proposed, which is shown in Fig. 10. Under acidic and neutral conditions, the CPC-PS exhibited a better BPA or DCP adsorption in their molecular forms, indicating almost no electrostatic attraction existing between the adsorbents and the pollutants. Based on the adsorption capacity, Zeta potential and content of element N of the CPC-PS and the PS, it could be validated that the CPC loading onto the PS was mainly ascribed to the electrostatic attraction between the cationic head-group and the negatively charged PS. In addition, the formation of CPC hemimicelles on the surface of PS could further enhance the adsorption capacity of PS for hydrophobic organic pollutants.

Considering that the PS contained a large amount of lignin, which endowed the CPC-PS with abundant benzene-ring structures, such benzene-ring structures could trigger the formation of π - π stacking between the adsorbents and the BPA and DCP. Besides, π - π stacking could also form between the pollutants within the hemimicelles, which would further enhance the adsorption process. The FT-IR spectra illustrate that the CPC-PS contained carboxyl, hydroxyl, and amide groups, which could adsorb both BPA and DCP from water through hydrogen binding. As a result, the enhancement mechanism of the CPC-PS for BPA and DCP adsorption was proposed and achieved mainly through three pathways, namely, the solubilization of hemimicelles for hydrophobic organic pollutants, the π - π stacking between benzene-ring structures, and the hydrogen bonding between the adsorbents and the pollutants.

Conclusions

This work used cationic surfactant CPC to modify PS as an effective adsorbent (CPC-PS) to remove hydrophobic BPA and DCP from water. Compared to the raw PS, the CPC-PS showed a superior adsorption performance. The BPA and DCP adsorption belonged to the pseudo-second-order kinetics, and fitted better to the Freundlich model. The BPA adsorption onto the CPC-PS was exothermic, while the DCP adsorption was endothermic. Regeneration of the CPC-PS using NaOH underscored a high applicability of this adsorbent. The primary enhancement mechanisms of the CPC-PS were proposed to be the solubilization of hemimicelles for hydrophobic organic pollutants, the π - π stacking between benzene-ring structures, and the hydrogen binding between the adsorbents and the pollutants. This work provides a cost-effective and high-efficient method to modify biomass wastes, and extends their reuse as adsorbents to remove hydrophobic organic pollutants.

Fig. 10 Proposed mechanism of BPA and DCP adsorption onto the CPC-PS



Author contribution Hefei Wang and Tian Tian designed and performed the research, and wrote the manuscript; Fangdi Xu reviewed and edited the manuscript; Dong Wang and Wei Ren analyzed the data; Dong Wang and Wei Ren acquired the funding. All authors read and approved the final manuscript.

Funding This study was supported by the Open Project of State Key Laboratory of Urban Water Resource and Environment, Harbin Institute of Technology (No.ES201605), and the Doctoral Scientific Research Foundation of National Marine Environmental Monitoring Center (No. 2021-Z-302).

Availability of data and materials All data generated or analyzed in this study are included in this published article.

Declarations

Ethics approval Not applicable.

Consent to participate Not applicable.

Consent for publication Not applicable.

Competing interests The authors declare no competing interests.

References

- Ayranci E, Duman O (2006) Adsorption of aromatic organic acids onto high area activated carbon cloth in relation to wastewater purification. *J Hazard Mater* 136(3):542–552
- Berhane TM, Levy J, Krekeler MPS, Danielson ND (2016) Adsorption of bisphenol A and ciprofloxacin by palygorskite-montmorillonite: effect of granule size, solution chemistry and temperature. *Appl Clay Sci*. 132–133:518–527
- Che Man SH, Ly D, Whittaker MR, Thickett SC, Zetterlund PB (2014) Nano-sized graphene oxide as sole surfactant in miniemulsion polymerization for nanocomposite synthesis: effect of pH and ionic strength. *Polymer* 55:3490–3497
- Cheng Q, Qu F, Li NB, Luo HQ (2012) Mixed hemimicelles solid-phase extraction of chlorophenols in environmental water samples with 1-hexadecyl-3-methylimidazolium bromide-coated Fe_3O_4 magnetic nanoparticles with high-performance liquid chromatographic analysis. *Anal Chim Acta* 715:113–119
- Chen T, Zhu ZL, Zhang H, Qiu YL, Yin DQ, Zhao GH (2020) Facile construction of a copper-containing covalent bond for peroxy-monosulfate activation: efficient redox behavior of copper species via electron transfer regulation. *ACS Appl Mater Interfaces* 12(38):42790–42802
- Cydzik-Kwiatkowska A, Zielinska M, Bernat K, Bulkowska K, Wojnowska-Baryla I (2020) Insights into mechanisms of bisphenol A biodegradation in aerobic granular sludge. *Bioresour Technol*. 315:123806

- Dehghani MH, Ghadermazi M, Bhatnagar A, Sadighara P, Jahed-Khaniki G, Heibati B, McKay G (2016) Adsorptive removal of endocrine disrupting bisphenol A from aqueous solution using chitosan. *J Environ Chem Eng* 4:2647–2655
- Ding H, Li X, Wang J, Zhang XJ, Chen C (2016) Adsorption of chlorophenols from aqueous solutions by pristine and surface functionalized single-walled carbon nanotubes. *J Environ Sci* 43:187–198
- Ge L, Kirumba G, Zhang B, Pal A, He YL (2015) Effect of surfactants on the removal and acute toxicity of aqueous nC(60) aggregates in water treatment process. *Environ Sci Pollut R* 22(13):9676–9685
- Huang GX, Wang CY, Yang CW, Guo PC, Yu HQ (2017) Degradation of bisphenol A by peroxymonosulfate catalytically activated with $Mn_{1.8}Fe_{1.2}O_4$ nanospheres: synergism between Mn and Fe. *Environ Sci Technol* 51:12611–12618
- Ibrahim S, Ang HM, Wang SB (2009) Removal of emulsified food and mineral oils from wastewater using surfactant modified barley straw. *Bioresour Technol* 100:5744–5749
- Jang HM, Yoo S, Choi YK, Park S, Kan E (2018) Adsorption isotherm, kinetic modeling and mechanism of tetracycline on *Pinus taeda*-derived activated biochar. *Bioresour Technol* 259:24–31
- Jiang J, Chen Y, Cao J, Mei C (2020) Improved hydrophobicity and dimensional stability of wood treated with paraffin/acrylate compound emulsion through response surface methodology optimization. *Polymers-Basel* 12:86
- Jin ZX, Wang XX, Sun YB, Ai YJ, Wang XK (2015) Adsorption of 4-n-nonylphenol and bisphenol-A on magnetic reduced graphene oxides: a combined experimental and theoretical studies. *Environ Sci Technol* 49:9168–9175
- Joseph L, Zaib Q, Khan IA, Berge ND, Park YG, Saleh NB, Yoon Y (2011) Removal of bisphenol A and 17 α -ethinyl estradiol from landfill leachate using single-walled carbon nanotubes. *Water Res* 45:4056–4068
- Jung C, Park J, Lim KH, Park S, Heo J, Her N, Oh J, Yun S, Yoon Y (2013) Adsorption of selected endocrine disrupting compounds and pharmaceuticals on activated biochars. *J Hazard Mater* 263:702–710
- Koopal LK, Goloub TP, Davis TA (2004) Binding of ionic surfactants to purified humic acid. *J Colloid Interf Sci* 275:360–367
- Kumar H, Katal A, Rawat P (2018) FT-IR spectroscopic and micellization studies of cetyltrimethylammonium bromide in aqueous and aqueous solution of ionic liquid (1-butyl-3-methylimidazolium bromide) at different temperatures. *J Mol Liq* 249:227–232
- Lin S, Zou CJ, Liang H, Peng H, Liao Y (2021) The effective removal of nickel ions from aqueous solution onto magnetic multi-walled nanotubes modified by β -cyclodextrin. *Colloid. Surface A* 619:126544
- Li Y, Jin FL, Wang C, Chen YX, Wang Q, Zhang WL, Wang DW (2015) Modification of bentonite with cationic surfactant for the enhanced retention of bisphenol A from landfill leachate. *Environ Sci Pollut R* 22:8618–8628
- Li Y, Liao XY, Huling SG, Xue T, Liu QZ, Cao HY, Lin QT (2019) The combined effects of surfactant solubilization and chemical oxidation on the removal of polycyclic aromatic hydrocarbon from soil. *Sci Total Environ* 647:1106–1112
- Marone A, Carmona-Martínez AA, Sire Y, Meudec E, Steyer JP, Bernet N, Trably E (2016) Bioelectrochemical treatment of table olive brine processing wastewater for biogas production and phenolic compounds removal. *Water Res* 100:316–325
- Meeker JD, Cantonwine DE, Rivera-Gonzalez LO, Ferguson KK, Mukherjee B, Calafat AM, Ye XY, Del Toro LVA, Crespo-Hernandez N, Jimenez-Velez B, Alshawabkeh AN, Cordero JF (2013) Distribution, variability, and predictors of urinary concentrations of phenols and parabens among pregnant women in Puerto Rico. *Environ Sci Technol* 47(7):3439–3447
- Moreman J, Lee O, Trznadel M, David A, Kudoh T, Tyler CR (2017) Acute toxicity, teratogenic, and estrogenic effects of bisphenol A and its alternative replacements bisphenol S, bisphenol F, and bisphenol AF in zebrafish embryo-larvae. *Environ Sci Technol* 51:12796–12805
- Mousset E, Oturan N, van Hullebusch ED, Guibaud G, Esposito G, Oturan MA (2014) Influence of solubilizing agents (cyclodextrin or surfactant) on phenanthrene degradation by electro-Fenton process – study of soil washing recycling possibilities and environmental impact. *Water Res* 48:306–316
- Mpatani FM, Han RP, Aryee AA, Kani AN, Li ZH, Qu LB (2021) Adsorption performance of modified agricultural waste materials for removal of emerging micro-contaminant bisphenol A: a comprehensive review. *Sci. Total Environ.* 780:146629
- Nagarajan R, Ruckenstein E (1991) Theory of surfactant self-assembly – a predictive molecular thermodynamic approach. *Langmuir* 7:2934–2969
- Nasar A, Mashkoo F (2019) Application of polyaniline-based adsorbents for dye removal from water and wastewater review. *Environ Sci Pollut R* 26:5333–5356
- Neris JB, Luzardo FHM, da Silva EGP, Velasco FG (2019) Evaluation of adsorption process of metal ions in multi-element aqueous systems by lignocellulosic adsorbents applying different isotherms: a critical review. *Chem Eng J* 357:404–420
- Ololade IA, Adeola AO, Oladoja NA, Ololade OO, Nwaolisa SU, Alabi AB, Ogungbe IV (2018) In-situ modification of soil organic matter towards adsorption and desorption of phenol and its chlorinated derivatives. *J Environ Chem Eng* 6:3485–3494
- Patel U, Parekh P, Sastry NV, Aswal VK, Bahadur P (2017) Surface activity, micellization and solubilization of cationic gemini surfactant-conventional surfactants mixed systems. *J Mol Liq* 225:888–896
- Peng H, Zou CJ, Wang CJ, Tang WY, Zhou JX (2020) The effective removal of phenol from aqueous solution via adsorption on CS/ β -CD/CTA multicomponent adsorbent and its application for COD degradation of drilling wastewater. *Environ Sci Pollut R* 27:33668–33680
- Pereira FV, Gurgel LVA, Gil LF (2010) Removal of Zn^{2+} from aqueous single metal solutions and electroplating wastewater with wood sawdust and sugarcane bagasse modified with EDTA dianhydride (EDTAD). *J Hazard Mater* 176:856–863
- Qiu PP, Zhao T, Zhu XH, Thokchom B, Yang JP, Jiang W, Wang LJ, Fan YC, Li XP, Luo W (2021) A confined micro-reactor with a movable Fe_3O_4 core and a mesoporous TiO_2 shell for a photocatalytic Fenton-like degradation of bisphenol A. *Chinese Chem Lett* 32:1456–1461
- Quan XC, Shi HC, Liu H, Lv PP, Qian Y (2004) Enhancement of 2,4-dichlorophenol degradation in conventional activated sludge systems bioaugmented with mixed special culture. *Water Res* 38:245–253
- Rehman A, Usman M, Bokhari TH, ulHaq A, Saeed M, Rahman HMA, Siddiq M, Rasheed A, Nisa MU (2020) The application of cationic-nonionic mixed micellar media for enhanced solubilization of Direct Brown 2 dye. *J. Mol. Liq.* 301:112408
- Ren DJ, Yu HY, Wu J, Wang ZB, Zhang SQ, Zhang XQ, Gong XY (2020) The study on adsorption behavior of 2,4-DCP in solution by biomass carbon modified with CTAB-KOH. *Water Sci Technol* 82:1535–1546
- Santos AP, Panagiotopoulos AZ (2016) Determination of the critical micelle concentration in simulations of surfactant systems. *J. Chem. Phys.* 144:044709
- Semerjian L (2018) Removal of heavy metals (Cu, Pb) from aqueous solutions using pine (*Pinus halepensis*) sawdust: equilibrium, kinetic, and thermodynamic studies. *Environ Technol Inno* 12:91–103
- Sun YF, Liu ZT, Fei ZH, Li CS, Chun Y, Zhang AM (2019) Synergistic effect and degradation mechanism on Fe-Ni/CNTs for

- removal of 2,4-dichlorophenol in aqueous solution. *Environ Sci Pollut R* 26(9):8768–8778
- Tian T, Zhou K, Li YS, Liu DF, Yu HQ (2020) Phosphorus recovery from wastewater prominently through Fe(II)-P oxidizing pathway in the autotrophic iron-dependent denitrification process. *Environ Sci Technol* 54:11576–11583
- Vandenberg LN, Hauser R, Marcus M, Olea N, Welshons WV (2007) Human exposure to bisphenol A (BPA). *Reprod Toxicol* 24:139–177
- Yin R, Shang C (2020) Removal of micropollutants in drinking water using UV-LED/chlorine advanced oxidation process followed by activated carbon adsorption. *Water Res.* 185:116297
- Yu JN, Zhu ZL, Zhang H, Di GL, Qiu YL, Yin DQ, Wang SB (2020) Hydrochars from pinewood for adsorption and nonradical catalysis of bisphenols. *J. Hazard. Mater.* 385:121548
- Zhou YB, Zhang RZ, Chen K, Zhao XR, Gu XC (2017) Enhanced adsorption and photo-degradation of bisphenol A by beta-cyclodextrin modified pine sawdust in an aquatic environment. *J Taiwan Inst Chem E* 78:510–516
- Zhou YB, Zhang RZ, Gu XC, Lu J (2015) Adsorption of divalent heavy metal ions from aqueous solution by citric acid modified pine sawdust. *Sep Sci Technol* 50:245–252

Publisher's Note Springer Nature remains neutral with regard to jurisdictional claims in published maps and institutional affiliations.